

PAPER • OPEN ACCESS

## Multiscale stress analysis of porosity clusters as mechanical models of degenerated graphite defects in cast iron

To cite this article: R Rizzoni *et al* 2022 *IOP Conf. Ser.: Mater. Sci. Eng.* **1214** 012035

View the [article online](#) for updates and enhancements.

You may also like

- [Void growth in high strength aluminium alloy single crystals: a CPFEM based study](#)  
Umair Asim, M Amir Siddiq and Murat Demiral
- [First Principles Model of Amorphous Silicon Lithiation](#)  
V. L. Chevrier and J. R. Dahn
- [Spatially-variant image-based modeling of PSF deformations with application to a limited angle geometry from a dual-panel breast-PET imager](#)  
Paul Gravel, Suleman Surti, Srilalan Krishnamoorthy et al.



The Electrochemical Society  
Advancing solid state & electrochemical science & technology

## 241st ECS Meeting

Vancouver, BC, Canada. May 29 – June 2, 2022



ECS Plenary Lecture featuring  
**Prof. Jeff Dahn,**  
**Dalhousie University**



Register now!



# Multiscale stress analysis of porosity clusters as mechanical models of degenerated graphite defects in cast iron

R Rizzoni\*, P Livieri and R Tovo

Department of Engineering, University of Ferrara, Via Saragat 1, 44122 Ferrara, Italy

\*Email: raffaella.rizzoni@unife.it

**Abstract.** We extend previous results for the stress analysis of a cluster of degenerated graphite in spheroidal cast iron, modelled as a multiscale three-dimensional composite. At the microscale, precipitates of degenerated graphite are modelled as spheroidal voids in a linear elastic matrix. At the mesoscale, clusters of degenerated graphite are aggregates of spheroidal voids. These aggregates are studied by means of a numerical analysis based on finite element simulations. As a second approach, the clusters are seen as homogeneous inclusions made of an equivalent porous elastic material. The average elastic properties of the porous material are calculated using an approach proposed by Tandon and Weng and based on Eshelby's equivalent principle and Mori-Tanaka's estimate. Comparison of the two approaches gives encouraging results in terms of average properties.

## 1. Introduction

Cast iron is an engineering material with a wide range of applications, such as turbines, pipes, machines, and automotive industry parts. In nodular cast iron, graphite spheroids or nodules provide large ductility and fatigue strength. Deviations from the spherical shape and arrangement of graphite particles are strongly related to temperature evolution and distribution during casting procedures and subsequent heat treatments. In thick-walled casted components, degenerated graphite microstructures frequently emerge resulting in deterioration of the mechanical properties [1-5].

In literature, ductile cast iron is often modelled as a composite material characterized by two phases: graphite nodules, acting as reinforcement, and the metal matrix. In this context, micromechanical modelling approaches have been proposed to understand the role played by graphite nodules during damage and failure [6-9]. In these works, cells models based on spherical or spheroidal graphite particles arranged regularly in a metallic matrix have been investigated. Graphite particles are frequently modelled as voids or cavities, because they are typically seen to undergo decohesion from the matrix, cf. [7,10,11].

For degenerated graphite, an approach treating graphite particles as porosity has been explored by the authors in [12-14]. In particular, at the microscopic scale, graphite precipitates are modelled as spheroidal voids, randomly oriented and orderly or disorderly distributed in a linear elastic isotropic matrix. The average elastic properties of the porous equivalent material can be evaluated numerically by the finite element (FE) method or analytically by means of Mori-Tanaka's (MT) estimate, as proposed by Tandon and Weng [15]. At a larger scale (mesoscale), a cluster of degenerated graphite is viewed as a single spheroidal inclusion embedded into the elastic isotropic matrix and made of



equivalent porous material. Eshelby's fundamental solution [16-18] is then applied to calculate the stress distribution internal and external to the inclusion modelling the cluster. Specifically, the proposed two-scale model allows characterizing average stress distribution inside the cluster depending on the following microstructure parameters: the density of graphite particles, their aspect ratio, the orientation and the aspect ratio of the cluster of degenerated graphite [13,14].

In the present paper, we extend our previous work in two ways. First, we compare the average elastic properties, calculated both numerically and analytically, with some experimental data available in the literature for porous materials. Next, we compare the results of external stress distribution calculated analytically (TW approach and Eshelby's solution) with those estimated numerically via FE simulations.

The plan of the paper is the following. Section 2 reviews the proposed multiscale model for cast iron with degenerated graphite. In Section 3, the experimentally calculated elastic properties of some porous materials are compared with the corresponding elastic properties calculated both numerically and analytically. Section 4 is devoted to the comparison between the results for stress analysis obtained via FE simulations and the average stress distribution calculated using the multiscale model. Some concluding remarks and future directions of the work are illustrated in Section 5.

## 2. Review of multiscale model for cast iron with degenerated graphite

Spheroidal cast iron is modelled as a composite material in which spheroidal voids with aspect ratio  $t$  (the ratio of length to semi-diameter) are randomly dispersed in a three-dimensional isotropic matrix.

At the microscale level of the composite, the average elastic properties of the porous equivalent material have been evaluated by using two different approaches: analytically, as proposed in [15,19], and numerically by the finite element (FE) method.

At the mesoscale level, for the analytical approach, a clusters of voids is described as a spheroidal inclusion having the average elastic properties calculated at the microscale. Numerically, clusters containing ordered and disordered distribution of randomly oriented spheroidal voids have been analyzed.

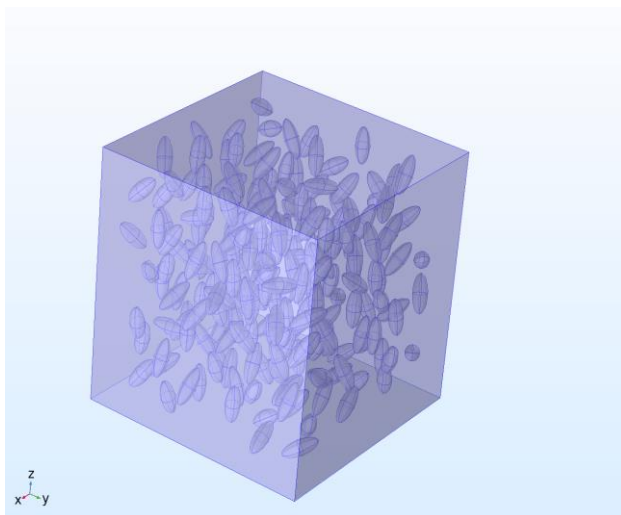


**Figure 1.** Example of microscale configuration numerically analyzed: disordered distribution of randomly oriented spheroids in a cube of  $L \times L \times L$  mm ( $L=6$  mm).

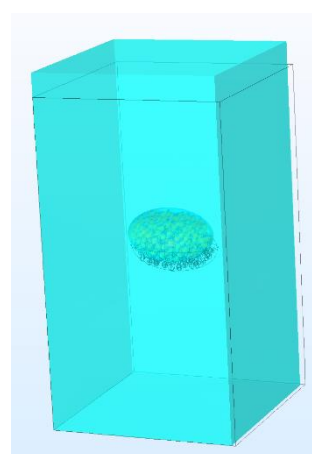


**Figure 2.** Example of mesoscale structure: cluster of spheroidal voids disorderly distribution inside a spheroidal volume.

### 2.1. Microscale level: porous material

Applying Eshelby's equivalent principle and Mori-Tanaka's hypothesis of the average stress in the matrix, Tandon and Weng have determined the average bulk and shear moduli of the equivalent porous material in terms of the porosity,  $\lambda$ , their aspect ratio,  $t$ , and the elasticity properties of the matrix [15,19]. From the estimated average bulk and shear moduli, the average Young modulus and Poisson ratio can be calculated under the assumption of macroscopically isotropic porous material. The latter assumption follows from the randomness of voids' orientations and it has been verified numerically.

In addition to the previous homogenization procedure, a three-dimensional FE analysis has been carried out using commercially available software (COMSOL Multiphysics). Cubes of linear elastic material with Young modulus and Poisson ratio  $E=206$  GPa and  $\nu=0.3$ , respectively, and ordered and disordered void distributions have been studied. The configuration shown in figure 1 represents a typical example. For the ordered distribution, randomly oriented voids are placed at the centers of a uniform grid with cube elementary cells of  $1 \times 1 \times 1$  mm. For the disordered distribution, the voids have centers placed randomly inside the volume and they do not overlap. For both types of distributions, the voids are spheroids with  $t$  ranging between 0.1 and 0.8.

### 2.2. Mesoscale level: a cluster of voids

A cluster of degenerated graphite is modelled as an inclusion perfectly bonded to an elastic three-dimensional matrix subjected to a given remote uniform load  $\sigma_0$ . The stress components inside and at the boundary of the inclusion have been calculated by applying Eshelby's solution [16-18].

Numerically, clusters of spheroidal voids have been tested in COMSOL under uniaxial tensile loading, as shown in figure 2. Inside the cluster, ordered and disordered distributions of voids have been taken into account.

## 3. Comparison with experimental data available in literature

The analytical and numerical estimates of average elastic properties calculated as summarized in Section 2 have been compared with the experimental results obtained in [20, 21]. In [20],  $20 \times 20 \times 150$  mm beams made of high strength hemihydrate plaster containing randomly distributed polystyrene agglomerates have been tested in four-point bending conditions. The content of polystyrene has been varied to realize different levels of porosity, which have been characterized by X-ray computed tomography and optical imaging on bidimensional sections. Typical load-displacement curves show a quasi-brittle behavior.

The elastic modulus  $\bar{E}$  is found to reduce with increase porosity and the following result (in GPa) was obtained in the regression analysis:

$$\bar{E} = 14.28 - 0.28 \lambda \quad (1)$$

with adjusted determination coefficient  $R^2 = 0.90$ . Figure 3 shows the graph of the relation (1), together with the estimate obtained by applying the Tandon and Weng approximation [15,19] and the numerical estimate obtained via the FE method. For both estimates, the porosity is modelled with disordered distributions of equal spherical voids.

Figure 3 indicates that the approach by Tandon and Weng and the numerical analysis of microstructures made of defects distributions are in good agreement with experimental data, with percent errors lower than 15% for porosity levels below 10%. For larger porosity values, the relative errors are found to increase. A possible reason may be the effect of the real pore microstructure, differing from the idealized distributions of spherical voids considered in calculating the estimates.

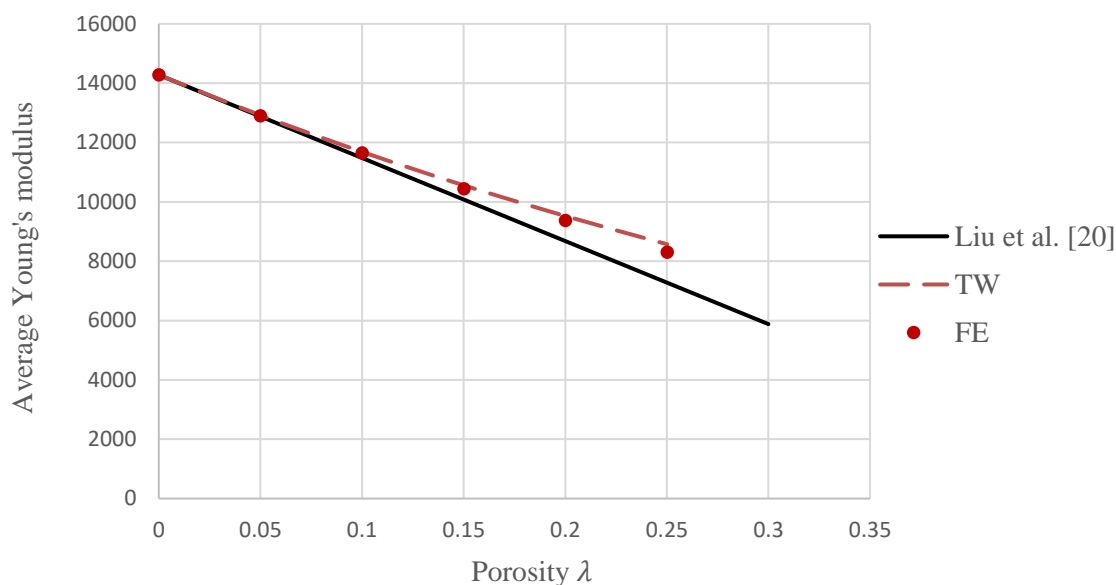


**Figure 3.** Average elastic modulus vs. porosity in a quasi-brittle porous material (see text for description). The black line corresponds to the linear regression calculated by Liu et al. with experimental data on beams in four point bending tests [20]. The dashed curve is the estimate obtained by applying the approach proposed by Tandon and Weng [15,19]. The dots correspond to the numerical estimate calculated analyzing disordered distributions of spherical voids.

In [21], Young's modulus of nodular cast iron  $\bar{E}_{ci}$  was measured by a pulse-echo elastic-wave technique. The volume fraction of the graphite nodules was determined by quantitative metallographic techniques. Several specimens were examined in three different conditions: as-cast (AC), annealed (A) and normalized-and-tempered (NT). Table 1 shows the experimentally measured values together with the estimates provided by the approximated method of Tandon and Weng (TW) and by the numerical analysis (FE). The two estimates were obtained by considering levels of porosity equal to the measured values of graphite volume fraction. For the considered values of the latter, the data listed in Table 1 indicate an excellent agreement between the experimental data and the analytical and numerical results.

**Table 1.** Average elastic modulus vs. porosity in nodular cast iron: comparison of model predictions with experimental data obtained from literature for cast iron in as-cast (AC), annealed (A) and normalized-and-tempered (NT) conditions [20].

Type	Graphite (%)	$\bar{E}_{ci}$ [20] (GPa)	TW (GPa)	FE (GPa)	Error TW (%)	Error FE (%)
AC	9.2	176.0	174.0	171.0	1.1	2.9
A	10.5	169.0	170.0	166.0	0.6	1.7
NT	9.2	169.0	174.0	171.0	2.9	1.2

#### 4. Validation of multiscale model via average stress distribution

To validate the multiscale model, the average stress distribution calculated analytically has been compared with the stress distribution calculated numerically in a porous spheroidal cluster under uniaxial tensile loading, as shown in Figure 2.

A rectangular box of dimensions 25×25×40 mm, with a cluster having semiaxes equal to 6 and 3 mm, has been numerically studied in COMSOL. Inside the cluster, the material is characterized by an ordered distribution of small spherical voids with a radius of 0.4 mm. The elastic constants of the matrix are as before,  $E = 206$  GPa and  $\nu = 0.3$ . Uniaxial traction was applied by imposing vanishing vertical displacement at the bottom surface of the box and a uniform distributed traction surface load  $\sigma$  at the top surface.

Table 2 shows the values of the stress components, averaged over the equatorial line of the spheroidal surface of the cluster and normalized with respect to the applied load  $\sigma$ . Table 2 shows also the normalized average values of the same stress components calculated by using the multiscale model, i.e. via Eshelby's solution at the external surface of the inclusion made of the equivalent porous material. The data listed in the Table indicate an overall good agreement between the two sets of average stress components. However, stress peaks strongly depending on relative position of neighbouring cavities cannot be detected by the multiscale model, in which defects are smeared out into equivalent porosity.

**Table 2.** Normalized average stress components calculated via a FE analysis performed over the porous cluster (label "FE") and via the multiscale model (label "MM"). The stress components are calculated over the equatorial line of the cluster's surface (for the FE model) and at the external surface of the inclusion (for the MM model), and they are averaged over the equatorial line and normalized with respect to the applied surface load  $\sigma$ .

Model	$\sigma_x/\sigma$	$\sigma_y/\sigma$	$\sigma_z/\sigma$	$\sigma_{xy}/\sigma$	$\sigma_{xz}/\sigma$	$\sigma_{yz}/\sigma$
FE	0.057	0.022	1.287	-0.002	-0.005	-0.010
MM	0.048	0.015	1.326	0.000	0.000	0.000

#### 5. Conclusion

In this paper, we have extended previous research on stress analysis in clusters of degenerated graphite in spheroidal cast iron, modelled as a multiscale three-dimensional composite. Clusters are viewed as spheroidal aggregates of spheroidal voids embedded in a three-dimensional linear elastic matrix. Two different approaches have been introduced: a numerical analysis based on finite element simulations and an analytical approach based on homogenization and Eshelby's solution. The two approaches are validated by comparing the predicted average elastic properties of the porous material inside the clusters with experimental data obtained from the literature [20]. A good agreement is observed, indicating that homogenization procedures are effective in estimating the elastic properties of spheroidal cast iron.

As a second validation, the stress components averaged over the equatorial line of the spheroidal surface of the cluster and normalized with respect to the applied load have been determined by either of two approaches. The comparison between the two sets of data indicates a good agreement. However, stress distribution calculated via FE analysis shows local stress peaks at the boundary of the cavities, strongly depending on their relative positions. These stress peaks cannot be detected by the analytical approach based on homogenization.

As a future development of the present model, extended approaches improving defects interactions should be explored, such as models based on Eshelby's formalism with polynomial eigenstrains [23]. Other issues to be explored could be the bonding and the damage of the graphite particles at the interface with the matrix, cf. [24-27].

## References

- [1] Hütter G, Zybell L and Kuna M 2015 *Eng. Fract. Mech.* **144** 118
- [2] Rausch T, Beiss P, Broeckmann C, Lindlohr S and Weber R 2010 *Procedia Eng.* **2** 1283
- [3] Costa N, Machado N and Silva F 2010 *Int. J. Fatigue* **32** 988
- [4] Lacaze J, Asenjo I, Mendéz S, Sertucha J, Larranaga P and Suárez R 2012 *Int. J. Metalcasting/Winter* 35
- [5] Kaczorowski J, Jozwiak K and Innocenti M 2013 *J. Fail. Anal. Prev.* **13** 445
- [6] Brocks W, Hao S and Steglich D 1996 *J. Phys.* VI **6** 43
- [7] Bonora N and Ruggiero A 2005 *Int J Solids Struct* **42** 1401
- [8] Bonora N, Gentile D, Ruggiero A and Iacoviello F 2003 *Proc. 9th Int. Conf. on the Mechanical Behaviour of Materials*, Genève, Swiss
- [9] Collini L and Nicoletto G 2005 *J. Strain. Anal. Eng.* **40** 107
- [10] Andriollo T, Thorborg J and Hattel J 2016 *Int. J. Solids Struct.* **100** 523
- [11] Dong M, Prioul C and François D 1997 *Metall. Mater. Trans. A* **28** 2245
- [12] Cova M, Livieri P, Rizzoni R and Tovo R 2017 *Procedia Struct. Integrity* **7** 446
- [13] Rizzoni R, Livieri P, Tovo R and Cova M 2020 *Theor. Appl. Fract. Mech.* **109** 102731
- [14] Rizzoni R, Livieri P and Tovo R 2021 *IOP Conf. Ser. Mater. Sci. Eng.* **1038** 012047
- [15] Tandon G P and Weng G J 1986 *Compos. Sci. Tech.* **27** 111
- [16] Eshelby J D 1957 *P. Roy. Soc. A-Math. Phys.* **241** 376
- [17] Eshelby J D 1959 *P. Roy. Soc. A-Math. Phys.* **252** 561
- [18] Eshelby J D 1961 in *Progress in Solid Mechanics*, eds. N Sneddon and R Hill vol. **2**, 89
- [19] Pan H H, Weng G J 1995 *Acta Mech* **110** 73
- [20] Liu D, Šavija B, Smith G E et al. 2017 *Int J Fract* **205** 57
- [21] Speich G R, Schwoeble A J and Kapadia B M 1980 ASME. *J. Appl. Mech.* **47** 821
- [22] Mura T 1987 *Micromechanics of Defects in Solids* (Springer Netherlands)
- [23] Fond C, Riccardi A, Schirrer R et al. 2001, *Eur. J. Mech. A/Solids* **20** 59
- [24] Lebon F, Dumont S, Rizzoni R et al 2016 *Compos. Part B-Eng.* **90** 58
- [25] Bonetti E, Bonfanti G, Lebon F and Rizzoni R 2017 *Meccanica* **52** 1911
- [26] Guinovart-Sanjuán D, Rizzoni R, Rodríguez-Ramos R et al 2017 *Compos. Struct.* **176** 539
- [27] Livieri P and Tovo R 2017 *Int. J. Fatigue* **101** 363